LuNART-q: The LuGRE Quick Navigation Analysis and Reporting Tool

LuNART-q: The LuGRE quick Navigation Analysis and Reporting Tool

Alex Minetto, Simone Zocca, Oliviero Vouch, Andrea Nardin, Fabio Dovis *Politecnico di Torino*
Mario Musmeci, Claudia Facchinetti, *Agenzia Spaziale Italiana (ASI)*

BIOGRAPHY

Alex Minetto received the B.Sc. (2013), M.Sc. (2015), and Ph.D. with honors (2020) in telecommunications and electrical engineering from Politecnico di Torino, where he is now Assistant Professor in the Department of Electronics and Telecommunications and a member of the NavSAS research group. His work focuses on advanced GNSS signal analysis, receiver design, and Bayesian state estimation. He has contributed to ESA and EUSPA projects and since 2021 has been involved in the Lunar GNSS Receiver Experiment (LuGRE) as a mission's Science Team member.

Simone Zocca received the B.Sc. (2018) in telecommunication engineering, the M.Sc. (2020) in communication and computer networks engineering, and the Ph.D. (2024) in electrical, electronics, and communications engineering from Politecnico di Torino. He is with the NavSAS Group, Department of Electronics and Telecommunications, working on innovative signal processing techniques and Bayesian estimation methods for GNSS.

Oliviero Vouch received the B.Sc. (2018) in electronics and communications engineering and the M.Sc. (2020) in communication and computer networks engineering from Politecnico di Torino, where he is currently pursuing a Ph.D. with the NavSAS Group, Department of Electronics and Telecommunications. His research focuses on advanced Bayesian estimation for multisensor integrated navigation systems based on GNSS.

Andrea Nardin received the M.Sc. (2018) and Ph.D. with honors (2023) in telecommunications and electrical engineering from Politecnico di Torino, where he is now Assistant Professor in the Department of Electronics and Telecommunications and a member of the NavSAS research group. In 2021, he was a Visiting Doctoral Researcher at Northeastern University, Boston. His research interests include signal processing architectures and signal design for GNSS and next-generation PNT systems.

Fabio Dovis received the M.Sc. (1996) and Ph.D. (2000) from Politecnico di Torino, where he is now Full Professor in the Department of Electronics and Telecommunications and coordinator of the NavSAS Research Group. His research focuses on GNSS receiver design, advanced signal processing for interference and multipath mitigation, and ionospheric monitoring. He has extensive experience in internation projects, collaborations with industry and research institutions, and serves on the IEEE AESS Navigation Systems Panel.

Mario Musmeci received a degree in physics from the University of Rome "La Sapienza." He has worked with major Italian space companies, ESA, and the European Commission on the Galileo program, and co-founded a start-up exploiting a patent based on Galileo signals for reliable traceability of "Made in Italy" products. Since 2016, he has been with ASI's Programs Directorate, serving as technical manager for LuGRE on NASA's Firefly Blue Ghost mission, demonstrating GNSS reception on the lunar surface.

Claudia Facchinetti is a researcher and technologist at the Italian Space Agency (ASI), specializing in Earth observation and space navigation technologies. She holds a Ph.D. in Space Science and Technology and has contributed to numerous scientific projects and space missions, including studies on SAR radar and hyperspectral sensors. She is a key member of the LuGRE (Lunar GNSS Receiver Experiment) team, a joint NASA-ASI initiative that successfully demonstrated GNSS-based navigation on the Moon during the Firefly Blue Ghost Mission 1 in 2025. Additionally, she is responsible for developing Earth observation missions at ASI.

ABSTRACT

The Lunar GNSS Receiver Experiment (LuGRE) quick Navigation Analysis and Reporting Tool (LuNART-q) is a MATLAB-based platform developed by Politecnico di Torino for the Italian Space Agency (ASI) and in collaboration with NASA's SCAN program and Qascom S.r.l. Derived from a broader scientific framework for the LuGRE mission, it enables rapid visualization, validation and exploitation of GNSS data acquired in lunar and cislunar environments. LuNART-q automates telemetry parsing, analysis and post-processing of GNSS observables and I/Q batch analysis, navigation performance evaluation, and structured reporting. Twelve configurable "quick experiments," derived from LuGRE Science Definition Team Report objectives, produce experiment reports that can be consolidated into operation

summary reports for immediate assessment. Visualization modules allow prompt analysis of signal availability, occultations, and receiver performance, while compliance with Ground System Working Group standards ensures interoperability. An open project based on LuNART-q will be released to allow the community to immediately explore LuGRE open data from the mission, fostering reproducibility, education, and collaborative research. By integrating predictive analysis, adaptive experiment execution, and reproducible reporting, LuNART-q provides an innovative framework that maximized the scientific return of the LuGRE mission and paves the way for companion software designed to support and advance scientific objectives in future missions.

I. INTRODUCTION

The Lunar GNSS Receiver Experiment (LuGRE) quick Navigation Analysis and Reporting Tool (LuNART-q) is a MATLAB-based software platform developed –to serve as a LuGRE mission tool– by the Navigation Signal Analysis and Research Group (NavSAS) within the Department of Electronics and Telecommunications of Politecnico di Torino. Research and development activities for the tool have been funded by Italian Space Agency (ASI) with the support of NASA's Space Communications and Navigation (SCAN) program with continuous feedback and refinements. LuNART-q has been derived from a broader framework, namely LuNART, which was conceived to enable the execution of extended scientific experiments identified in the context of the LuGRE mission by the mission Science Team through the LuGRE Science Definition Team report (SDTR) (Konitzer et al., 2024).

LuGRE quick navigation analysis and reporting tool (LuNART-q) was specifically designed to support both the preparatory and post-operational phases of the LuGRE mission, a collaborative initiative involving National Aeronautics and Space Administration (NASA), ASI, and Qascom s.r.l. to demonstrate the usability of global navigation satellite system (GNSS) signals in cislunar and lunar environment (Parker et al., 2022; Tedesco et al., 2023). LuNART-q addresses the critical need for early-stage assessment of scientific integrity of mission data, mission scientific return, and reproducibility of mission data analyses by the scientific community. Besides, it enabled an effective validation of scientific results from the very first phases of the mission.

Unlike existing GNSS post-processing tools, LuNART-q provides a comprehensive, automated, and structured approach to mission's GNSS data validation, scientific experiment execution, and prompt reporting for time-critical operations and procedures. It is designed to handle raw GNSS observables and in-phase/quadrature signal batches from Global Positioning System (GPS) and Galileo L1/E1 and L5/E5a bands, and compare them to the predicted scenarios into a cohesive framework, ensuring scientific data integrity and usability throughout the mission lifecycle and for the open release to the community by October 2025.

Its modular and flexible architecture supports structured sessions for each mission operation, automated or manual configuration of experiments according to the specificity of mission operations, and the execution of 12 configurable quick scientific experiments per mission operation, derived from the SDTR experiments foreseen by the LuGRE's Science Team. Each experiment generates a quick experiment report (QER), which can be consolidated into an operation summary report (OSR) to provide an operation-wide assessment of performance and scientific insights right after operations completion.

LuNART-q further distinguishes itself through its advanced workflow, which automates mission analysis, supports prompt processing of captured GNSS data and raw signal batches collected throughout the mission, and enables adaptive experiment reconfiguration through dedicated settings. Core functionalities include payload telemetry parsing, GNSS observable analysis and post-processing, onboard navigation solution analysis via a weighted least squares (WLS) estimator, and automated handling of operational metadata. Integrated visualization modules allow to infer GNSS signal availability, ionospheric crossings, Earth and lunar occultations, and receiver state estimation. Signal probes and spectral analysis provide time-frequency visualization of I/Q batches, interference detection, and analog-to-digital converter (ADC) integrity monitoring. Compliance with Ground System Working Group (GSWG) guidelines ensures seamless file detection, local storage, and data exchange between payload and ground segments.

Partly inspired by Google Analysis Tools for GNSS raw measurements (Fu et al., 2020), LuNART-q emphasizes automation, flexibility, and accessibility, reducing data processing overhead for both mission operators and researchers in the field lunar GNSS research. Its procedural workflow includes four stages:

1. Prediction analysis and report generation, producing prediction evaluation report (PER) to optimize signal reception timespan of each mission operations;
2. Session Configuration, enabling automated or manual selection of operations, users, and reference data;
3. Scientific experiment execution, generating QER based on GNSS data analysis;
4. Comprehensive Mission Summary, compiling OSRs to evaluate performance and propose corrective actions.

Beyond its operational role in LuGRE, LuNART-q offers a flexible experimental framework for Lunar GNSS navigation research. Its MATLAB-based modular design allows integration of additional functionalities, promoting educational and research opportunities within the GNSS community (Hossain, 2022). By combining rapid data analysis, structured reporting, predictive evaluation, and adaptive experiment execution, LuNART-q represents an innovative tool for advancing space-based navigation methodologies and assessing lunar GNSS mission performance.

Fig. 1a shows the splash-screen of the MATLAB standalone application including mission logo (top-right), developers and partners logos (bottom). A detail of LuNART-q logotype with its distinctive elements is reported in Fig. 1b.

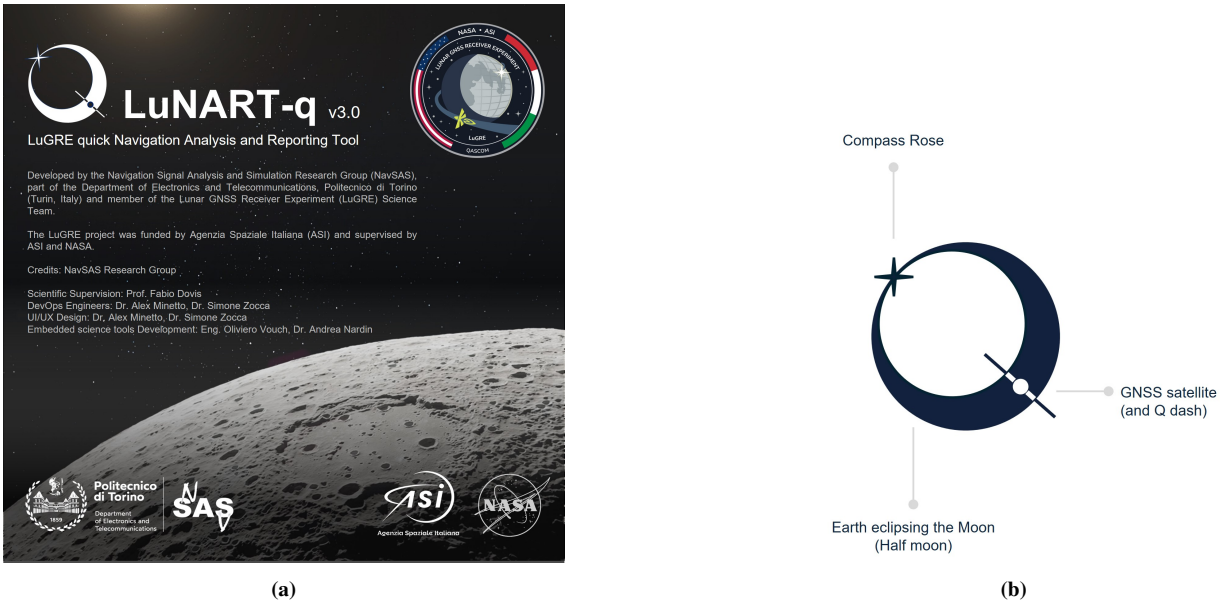

(a) **(b)**

Figure 1: LuNART-q v3.0 MATLAB application splashscreen and logotype.

II. PAPER ORGANIZATION

The manuscript includes a discussion about requirements and functionalities of the software in Section III; LuGRE mission quick-look experiments are described in Section IV. Conclusions and further development are drawn in Section V and VI, respectively.

III. SOFTWARE ARCHITECTURE AND GRAPHICAL USER INTERFACE

The LuNART-q software architecture is based on a set of software functionalities designed to implement specific project requirements. The mapping between functionalities and requirement is detailed in Tab. 1.

1. Back-end: Logical architecture

The LuNART-q consists of a main function of the format ".mlapp", which contains all the properties of graphical user interface (GUI) elements and their related callbacks. The callbacks then point to other Matlab scripts in order to perform most tasks, e.g., parsing, plotting and generating reports. The various functions are contained in different subfolders in the *library* folder, depending on their purpose.
Each experiment is associated to at least one plotting function, and each plotting function is called by at least one experiment. This structure allows for modular design of experiments, where plots can be easily added, moved or deleted from experiments. Each plotting function has a similar structure and takes as input the data needed for plotting, as well as various settings and flags used to generate the plot and correctly displaying the title and axis labels.

2. Front-end: Graphical user interface

The LuNART-q is composed of three main tabs:

1. Home tab (session configuration)

Table 1: Mapping of LuNART-q functionalities to LuGRE's science operations requirements.

Requirement	Implemented Functionalities
Ingesting I/Q batches and telemetry data for each operation, the latter of which needs to be parsed before being ready for scientific analysis	• Full data workflow supporting SPC operator sessions • Automatic file detection based on the mission folder structure (GSWG standard) • Session configuration panel with automatic pre-filling of metadata from the mission scheduler. • Processing modes: standard, custom, or single-experiment OPS windows • Integration and time alignment of predicted data from dedicated mission planner
Allowing Science Team operators (SPC-O) to perform quick-look scientific experiments in a reasonable timespan	• Execution of all rapid scientific experiments (Q1.a–Q3.b), including condensed SDTR experiments • Evaluation mode for predicted data (preparatory use) • Simplified configuration panel for quick setup • Operator identification inherited from Windows user account.
Storing the results and generating a report of each scientific experiment	• Report formats including operation metadata, tagging options, and differentiation by institutions' locations • Automatic generation of the OSR, consolidating selected results across multiple sessions
Transferring the results and reporting to the Payload Operations Center (POC) File Depot for prompt consultancy during OPS	• Automatic generation of rapid reports for immediate use. • OSR functionality consolidates key outputs for transfer to the POC.

2. Scientific experiments tab
3. Summary report tab

The home tab, depicted in Fig. 2a, contains the following items

1. A set of GUI elements used to parse the data of an operation and display the associated mission operation metadata
2. A text box with information regarding all user activities and error messages. The content is also saved into a log `.txt` file continuously appended every time the LuNART-q is operated.
3. A set of lamps used to display the current status of the LuNART-q, i.e., whether data has been parsed successfully or whether the experiments can be run.
4. A set of GUI elements used to parse, run and generate a report for dedicated mission planner and prediction generator, i.e., NASA's Goddard Enhanced Onboard Navigation System (GEONS).

The experiments tab contains, in turn, another tab group, in which any tab corresponds to a scientific experiment, as shown in Fig. 2b. Each experiment sub-tab contains a textual description of the experiment and its output. Similarly to the main tab, is also contains a text box with information about the current status of the experiment. The workflow for each experiment is as follows; first the user selects the settings (if any), then the experiment is run, then the plots are saved and a report is generated, and finally the folder containing the results is sent to the POC. Each of these steps is associated with a button that is enabled only if the previous step was completed successfully.

Nonetheless, the operator may decide to stop at any point. For example, if the results of the experiment are unsatisfactory, the user may decide to run the experiment again with different settings before saving the results. The user may also save more then one set of results for the same experiment, which are then identified by means of a counter. Each experiment of each operation has an associated counter tracking the number of times results have been saved for that particular experiment on that sat of data. This counter is also used to name the folder where results are stored.

Finally, the summary report tab is used to assemble an operation-wide report containing at most one report per experiment. For example, if the receiver did not perform its state estimation during the operation, experiments associated to this specific experiment cannot be performed and their report will not appear in OSR for that operation.

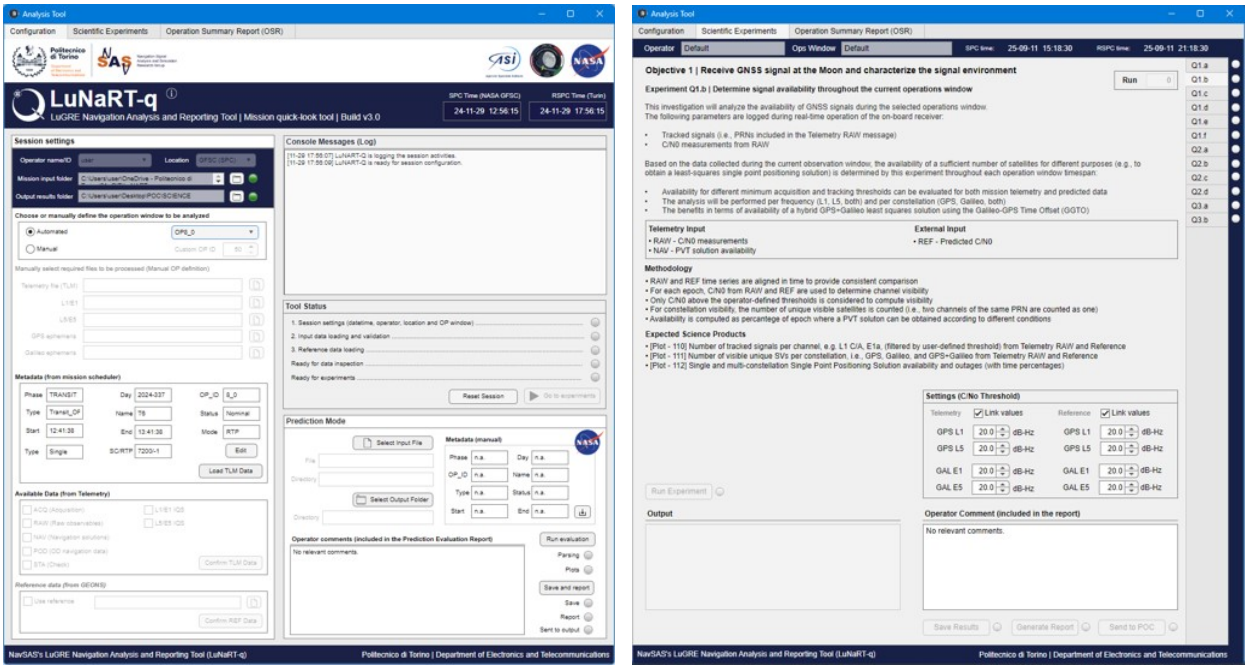

(a) Home tab (session configuration) **(b)** Quick experiment tab

Figure 2: LuNART-q v3.0 graphical user interface (MATLAB standalone app under Windows 11).

IV. QUICK SCIENTIFIC EXPERIMENTS

The extended scientific experiments of the LuGRE mission were structured around three main objectives: (1) to receive GNSS signals at the Moon, return the data to Earth, and characterize the lunar GNSS signal environment; (2) to demonstrate navigation and time estimation using the collected GNSS data; and (3) to exploit such data in support of the development of GNSS receivers tailored to lunar operations. In line with these objectives, the set of LuNART-q experiments designed for implementation within LuNART-q have been organized and presented accordingly, through the following subsections.

All the quick experiments relies on a set of predefined input data:

- RAW: Raw GNSS mesasurements as observed from on-board receiver tracking channels
- NAV: Navigation solutions estimated through a WLS algorithm.
- POD: Navigation solutions estimated through an extended Kalman Filter integrating orbital dynamics model.
- REF: Reference data provided from planning and predictions tool (i.e., GEONS).
- IQS: I/Q signal batch collected by the receiver.
- EPH: GNSS broadcast ephemeris.

The specific datasets and time series associated with each category are reported in the respective descriptive tables of the experiments that follow. All data listed above, except for POD and REF data, will be publicly released by October 2025 in an adapted data formats.

1. Objective 1: Receive GNSS signal at the Moon and characterize the signal environment

a) Q1.a Measure the signal strength (C/No) throughout the current operations window

This investigation uses the LuGRE receiver to measure signal strength, i.e., carrier-to-noise density Ratio (C/No) from radiometrically-visible GNSS satellites. This investigation focuses on receiver-reported C/No as a proxy for received signal power. C/No mission telemetry time series are compared to predicted C/No data (if any available).Table 2 summarizes the experiment's inputs, outputs, and methodology.

b) Q1.b Determine signal availability throughout the current operation window

This investigation analyses the availability of GNSS signals during the current operations window. The following parameters are logged during real-time operation of the on-board receiver:

Table 2: Overview of C/N_0 data processing and expected products.

Category	**Details**
Telemetry Input	RAW – Measured C/N_0
External Input	REF – Predicted C/N_0
Methodology	• RAW and REF time series are aligned in time to provide consistent comparison by means of REF polynomial interpolation. This is done for every experiment that compares telemetry and reference data.
Expected Science Products	• Figure 100: RAW – Measured C/N_0 time series • Figure 101 (optional): REF – Predicted C/N_0 time series • Figure 102 (optional): Difference of C/N_0 time series (common visibility between RAW and REF)

- Tracked signals identified by signals bands (i.e., L1/E1, L5E5a) and PRNs included in the telemetry RAW message
- C/No measurements from RAW

Based on the data collected during the current observation window, the availability of a sufficient number of satellites for different purposes (e.g., to obtain a least-squares, single-point navigation solution) is determined by this experiment within each operation window's timespan.

Availability for different minimum acquisition and tracking thresholds can be evaluated for both mission telemetry and predicted data. The analysis is performed per frequency (L1/E1, L5/E5a or both) and per constellation (GPS, Galileo or both). The benefits in terms of availability of a multi-constellation least squares solution using the Galileo-GPS Time Offset (GGTO) is inferred through this experiment. Tab. 3 summarizes the experiment's inputs, outputs, and methodology.

Table 3: Overview of signal visibility and availability data processing and expected products.

Category	**Details**
Telemetry Input	RAW – Measured C/N_0
External Input	REF – Predicted C/N_0
Methodology	• C/No time series from RAW and REF are used to determine channel visibility • Only C/No value above the operator-defined thresholds is considered to compute radiometric visibility at the receiver • For constellation visibility, the number of unique visible satellites is counted (i.e., two channels, e.g., L1 C/A, L5 transmitted by the same satellite vehicles are counted as one) • Availability is computed as percentage of epoch where a least squares (LS) state estimation solution can be obtained according to different conditions
Expected Science Products	• Figure 110: Number of tracked signals per channel (filtered by user-defined threshold) from NAV and REF • Figure 111: Number of visible unique satellite vehicles per constellation from NAV and REF • Figure 112: Single and multi constellation availability and outages (with time percentages) for single point positioning solution
Configuration	C/No threshold per constellation and channel

c) Q1.c: Measure pseudorange from visible satellites throughout the current operations window

This investigation exploits the LuGRE payload to collect pseudorange measurements from tracked GNSS satellites signals throughout the selected operations window.

In-flight pseudorange measurement collection is a precursor to generating onboard and ground-based navigation solutions via least squares estimator and to initialize Bayesian navigation filters (e.g., extended Kalman filter); such use cases are addressed in investigations Q2.a, Q2.b, Q2.c and Q3.a. Tab. 4 summarizes the experiment's inputs, outputs, and methodology.

Table 4: Overview of pseudorange data processing and expected products.

Category	**Details**
Telemetry Input	RAW – Code pseudorange measurements
External Input	REF – Predicted ranges
Methodology	• Uncorrected pseudoranges are used from payload telemetry (RAW), while geometrical ranges are used from the reference (REF)
Expected Science Products	• Figure 120: RAW - Raw code pseudorange times series • Figure 121 (optional): REF - Predicted code pseudorange times series • Figure 122 (optional): Difference of code pseudorange time series (common visibility)

d) Q1.d: Evaluate pseudorange error from visible satellites throughout current operations window

This investigation analyses pseudorange deviations from the expected value for tracked GNSS satellites signals by comparing the measured values (corrected with the receiver clock bias) with the predicted ranges. Differently from experiment Q1.c (which only reports on-board raw pseudorange measurements), this experiment aims at providing a statistical characterization of their deviations throughout the operations window. The deviation is characterized in terms of mean (error bias) and standard deviation of the measurements noise.

The experiment is performed on both code and phase pseudoranges. Tab. 5 summarizes the experiment's inputs, outputs, and methodology.

e) Q1.e: Measure Doppler-shift and Doppler-rate profiles throughout the current operations window

This investigation utilizes the data collected by the LuGRE receiver to depict Doppler shift and Doppler rate profiles of visible GNSS satellites during the transit operational periods and on the lunar surface. Tab. 6 summarizes the experiment's inputs, outputs, and methodology.

f) Q1.f: Evaluate the presence and characteristics of multipath due to the Blue Ghost lander and/or the lunar surface

This investigation aims at identifying potential anomalies affecting GNSS observables due to multipath phenomena. Multipath typically induce biases in both DLL and PLL thus leading to biased pseudorange measurements. The experiment is based on the post-processing of multi-frequency code and carrier-phase pseudorange measurements through Code-minus-Carrier (CMC) approach and its variants.

Multi-frequency code and phase pseudorange observables time series are subtracted. The combination of multi-frequency measurements allows to remove any potential ionospheric contribution. The technique clusters three remaining errors terms:

- Composite multipath
- Carrier-phase ambiguity
- Composite receiver noise

When unsmoothed code measurements are employed, phase multipath and noise terms are assumed negligible w.r.t. to the code counterparts. The resulting CMC time series can be eventually detrended by subtracting its mean through a sliding mean (default) approach, thus removing piece-wise constant terms. Tab. 7 summarizes the experiment's inputs, outputs, and methodology.

Table 5: Overview of pseudorange error characterization and expected products.

Category	Details
Telemetry Input	• RAW – Code pseudorange measurements • RAW - Phase pseudorange measurements • NAV - Bias of the receiver clock
External Input	REF – Predicted ranges
Methodology	• The plot shows the difference between RAW pseudoranges corrected with estimated receiver clock bias and the reference predicted ranges • If a reference is not available, the method of finite differences is used to compute the third derivative (with 4th order of accuracy) to remove trends from the measurements due to relative dynamics between the lander and GNSS satellites. • Mean and standard deviation are computed from the time-series and shown in a table
Expected Science Products	• Figure 130: If reference is available, range error time series plot (difference between REF predicted range and RAW raw pseudorange corrected by NAV clock bias). Otherwise, third-order finite difference of pseudoranges is displayed • Figure 131: third-order finite difference of phase pseudoranges • Table: Estimated measurement noise bias and standard deviation from Plot 130 and 131

Table 6: Overview of Doppler shift and Doppler rate data processing and expected products.

Category	Details
Telemetry Input	• RAW - Doppler shift measurements • RAW - Doppler rate measurements
External Input	• REF – Predicted Doppler shift • REF - Predicted Doppler rate
Methodology	• Doppler shift and Doppler rate time series are plotted both from RAW and REF sources
Expected Science Products	• Figure 140: RAW - Doppler shift time series • Figure 141 (optional): REF - Predicted Doppler shift time series • Figure 142: RAW - Doppler rate time series • Figure 143 (optional): REF - Predicted Doppler rate time series • Figure 144 (optional): Difference of Doppler shift time series (common visibility) • Figure 145 (optional): Difference of Doppler rate time series (common visibility)

Table 7: Overview of code-minus-carrier characterization and expected products.

Category	Details
Telemetry Input	• RAW - Raw pseudorange measurements • RAW - Carrier phase measurements
External Input	n.a.
Methodology	• For epochs in which multi-frequency measurements are available, a dual frequency code-minus-carrier (CMC) is computed • The operator can choose to plot either the original or de-trended (mean-subtracted) CMC time series • The experiment calculates the mean and standard deviation using a rolling window of size selected by the operator • The operator can also select a threshold for outliers, defined as multiples of the estimated standard deviation • Samples that overcome the threshold are highlighted in plots and collected as potential outliers in the tables
Expected Science Products	• Figure 160: CMC or detrended CMC time series • Figure 161: CMC or detrended CMC with overlapping outliers' detection • Table: RAW - Outliers value and location per each signal
Configuration	• Code-minus-carrier technique • Window size for standard deviation estimation • Standard deviation threshold for outliers detection

2. Objective 2: Receive GNSS signal at the Moon and characterize the signal environment

a) Q2.a: Calculate and Characterize Least Squares, Multi-GNSS, single point solutions throughout the mission

This investigation estimates the BGM1 lander state vector (position, velocity, clock bias), and its associated uncertainties from real-time GNSS observables using the LuGRE receiver's onboard implementation of a least squares multi-GNSS point solution. This investigation has the following outcomes:

- Demonstrates real time onboard least squares positioning in transit, near the Moon and on the lunar surface.
- Demonstrates multi-GNSS least-squares solution beyond the Space Service Volume (SSV).
- Characterizes achieved precision and accuracy onboard and in post-processing (see also investigation Q3.a)

Tab. 8 summarizes the experiment's inputs, outputs, and methodology.

b) Q2.b: Calculate and Characterize Kalman-filter based navigation solutions on-board (transit and surface)

This investigation utilizes the LuGRE receiver's onboard extended Kalman filter to process real-time GNSS observables and generate a sequential estimate of the BGM1 lander position, velocity, time, and the associated uncertainties. This experiment is intended to directly demonstrate filter-based navigation in the lunar regime, especially during intervals in which signal availability does not allow for filter re-initialization with new single-point solution. Such usage is expected to be the primary use case for GNSS in the lunar vicinity.

This investigation has the following outcomes:

- Demonstrates real-time onboard filter-based navigation in transit, near the Moon and on the lunar surface.
- Demonstrates multi-GNSS filter-based navigation in the SSV.
- Characterizes navigation solution achieved accuracy. When available, it compares availability and accuracy to least squares point solutions (see investigation Q2.c).

This investigation is applicable to both transit and surface phases. Each phase uses a specialized algorithm specific to

Table 8: Overview of receiver state estimation data processing and expected products.

Category	Details
Telemetry Input	NAV - Position, Velocity and Clock bias estimates
External Input	REF – Predicted trajectory
Methodology	• The experiment provides a visualization of the solutions obtained onboard and associated uncertainties • The operator can choose which reference frame to use for the plots (ECI of ECEF)
Expected Science Products	• Figure 200: NAV - On-boad estimated position time series (per-axis subplots) compared to reference data (if available) • Figure 201: NAV - On-boad estimated velocity time series (per-axis subplots) compared to reference data (if available) • Figure 202: NAV - On-boad estimated clock bias and clock drift time series • Figure 203: NAV - On-boad estimated standard deviations (subplots for position, velocity and time estimates)

its dynamics environment. Tab. 9 summarizes the experiment's inputs, outputs, and methodology.

Table 9: Overview of filter-based state estimation data processing and expected products.

Category	Details
Telemetry Input	POD - Position, velocity and clock bias estimates
External Input	REF – Predicted trajectory
Methodology	• The experiment provides a visualization of the solutions obtained onboard and associated uncertainties • Position and velocity standard deviations are computed as the square root of the trace of the associated uncertainty matrices
Expected Science Products	• Figure 210: POD - On-board estimated position time series (per-axis subplots) • Figure 211: POD - On-board estimated velocity time series (per-axis subplots) • Figure 212: POD - On-board estimated clock bias and clock drift time series • Figure 213: POD - On-board estimated standard deviations (subplots for position, velocity, clock bias and clock drift estimates)

c) Q2.c: Characterize position, velocity, and time uncertainty and convergence properties throughout mission

This investigation further characterizes the uncertainty associated with the position, and velocity estimates from the payload onboard navigation filter. Specific characterizations include:

- Position and velocity estimation error
- Comparison of filter error with estimated standard deviation

This investigation performs comparisons between filters used onboard and a reference trajectory. Tab. 10 summarizes the experiment's inputs, outputs, and methodology.

d) Q2.d: Compute the Dilution of precision from received signals when available

The dilution of precision (DOP) identifies a coefficient that regulates the measurements error propagation as a mathematical effect of the relative geometry between observed GNSS satellites and receiver location. It is computed through

Table 10: Overview of receiver state estimation error characterization, related data processing and expected products.

Category	Details
Telemetry Input	• NAV - Position and velocity estimates with standard deviations • POD - Position and velocity estimates with standard deviations
External Input	• REF - Predicted states (no clock bias) • EPH - GPS and Galileo ephemerides
Methodology	• The experiment takes telemetry NAV and POD data and provides a plot of their error w.r.t. reference trajectory from REF • Position and velocity standard deviations from POD are computed as the square root of the trace of the associated uncertainty matrices • If REF trajectory is not available, the difference between the filter estimates is visualized instead
Expected Science Products	• Figure 220: NAV and POD - If reference is available, 3D position error time series of both NAV and POD is plot (ECI frame) along with standard deviation estimated by the filters. Otherwise, 3D position difference between Telemetry NAV and POD is shown • Figure 221: NAV and POD - Same as plot 210 but for Velocity instead

Jacobian of the set of equations describing the linearized multi-lateration problem. As such, it is calculated based on the position of the satellites used for the fix and the true position of the user (or of a linearisation point sufficiently close to it) and does not depend on the accuracy of the measurements, nor on the selected reference frame.

Under the assumption of zero-mean, independent and identically distributed (i.i.d.) Gaussian measurement errors, the root mean square (RMS) error of the state estimates can be written as the product of the GDOP and the standard deviation of the measurements noise.

This experiment aims at

- Collecting the Geometrical dilution of precision (DOP), Position DOP, and time DOP values computed by the on-board receiver and compare them to predicted values.
- Use the outputs of investigations 1.d (standard deviation of the pseudorange error measurements), 2.a (point solution), and 2.b (filter solution) to verify the relationship between pseudorange measurement error and the receiver-computed geometric dilution of precision (GDOP), position dilution of precision (PDOP) and time dilution of precision (TDOP).

Tab. 11 summarizes the experiment's inputs, outputs, and methodology.

3. Objective 3: Compute the Dilution of precision from received signals when available

a) Q3.a: Process GNSS observables to assess achievable onboard navigation performance

This investigation performs post-processing of pseudorange and pseudorange rate measurements retrieved by the LuGRE payload with different estimation algorithms to evaluate achievable receiver state estimation performance regardless of the on-board implementation and solution.

The experiment provides a benchmark to assess the on-board navigation performance against potentially achievable performance. Beyond a further assessment and validation of the on-board navigation solution, this experiment supports trade-offs between different filter algorithms and configurations to support the development of lunar-focused real-time filters.

The quick-look implementation foresees the processing of GNSS observables by means of

- WLS state estimation algorithm

Table 11: Overview of DOP metrics data processing and expected products.

Category	Details
Telemetry Input	NAV - GDOP, PDOP, TDOP
External Input	REF - Predicted GDOP, PDOP, TDOP
Methodology	• Since the receiver does not acquire all satellites at once, the number of tracked signals at the beginning of each dataset may be very low, thus leading to large DOP values. The operator can decide too skip the beginning of the dataset for the sake of a meaningful visualization
Expected Science Products	• Figure 230 (a): DOP metrics time series from NAV (along with REF if available) • Figure 230 (b): Overall number of tracked signals (channels) from NAV
Configuration	Starting epoch

- extended Kalman filter (EKF) initialized by WLS early estimates

Tab. 12 summarizes the experiment's inputs, outputs, and methodology.

Table 12: Overview of post-processing state estimation data processing and expected products.

Category	Details
Telemetry Input	• RAW - Code pseudorange measurements • (Optional) RAW - Phase pseudorange measurements • RAW - Doppler shift measurements • NAV - Position, Velocity and Clock bias estimates
External Input	• REF - Predicted trajectory • EPH - GPS and Galileo ephemeris
Methodology	• Perform receiver state estimation relying on the input measurements and ephemeris data
Expected Science Products	• Figure 300: Post-processing estimated position time series (per-axis subplots) compared to reference data (if available) • Figure 301: Post-processing estimated velocity time series (per-axis subplots) compared to reference data (if available) • Figure 302: Post-processing estimated clock bias and clock drift time series • Figure 303: Post-processing estimated standard deviations (subplots for position, velocity and time estimates)

b) Q3.b: Process GNSS I/Q samples with independent software/hardware receivers

This investigation assesses the replicability of onboard receiver's GNSS signal processing (at radio-frequency level) by leveraging multi-frequency I/Q signal batches collected by the LuGRE payload during dedicated sample capture operations. A time-frequency analyzer is in charge of providing an overview of signal characteristics while an acquisition routine is in charge of post-processing the batches both for L1/E1 and L5/E5a to identify acquirable signals and estimate their code phase and frequency offsets. Different configurations parameters are available to optimize

acquisition performance. This quick investigation supports:

- An analysis of possible signal distortions due to unexpected dynamics of the signals, by means of estimated probability densities of samples.
- An analysis of the spectral behaviour and presence of potential outliers due to propagation environment, radio-frequency interferers or front-end failures.
- An assessment of the telemetry data obtained on-board during subsequent real-time operations (i.e., initial ACQ C/No and Doppler shift estimate).

Tab. 13 summarizes the experiment's inputs, outputs, and methodology.

Table 13: Overview of I/Q samples data processing and expected products.

Category	**Details**
Telemetry Input	• I/Q samples batch • ACQ - PRN of acquired satellites • ACQ - C/No measurements • ACQ - Doppler shift measurements
External Input	n.a.
Methodology	• The acquisition stage processes the initial 50 ms of the IQS batch to provide time-domain and frequency-domain analysis. • I/Q samples are used to estimate C/No and Doppler shifts, which are compared to the ACQ counterparts obtained by the payload operating in mixed mode
Expected Science Products	• Figure 310: Probe data including 50 ms time-series, histogram of quantized values, samples distribution with Gaussian fit check • Figure 311 and 313: Acquisition results with estimated C/No for L1 and E1 respectively • Table 312 and 314: Comparison of on-board estimated C/No and Doppler shift (from ACQ data) and post-processed outcomes for L1 and E1 respectively
Configuration	• Doppler search space size, centre offset and step size • Coherent integration time • Non-coherent sums • False alarm probability • Use of Doppler-affected code

V. CONCLUSION

LuNART-q provides a versatile MATLAB-based platform for the rapid validation and analysis of GNSS data collected during the LuGRE mission, seamlessly integrating telemetry parsing, I/Q batch processing, and post-processing of multi-constellation GNSS observables. The tool enables automated execution of quick scientific experiments and generation of structured reports, supporting both operational assessment and post-processing. It allows quantitative characterization of lunar GNSS signals, including C/N_0, availability, pseudorange, Doppler shift, and multipath metrics, and demonstrates onboard and post-processed multi-GNSS navigation solutions beyond the terrestrial Space Service Volume. With a modular, user-friendly interface and full traceability of operator actions, LuNART-q ensures reproducibility, and interoperability with ground systems, providing a robust framework to accelerate data exploitation and advance lunar navigation research.

VI. FURTHER WORKS

The LuNART project, once released as open-source through an open GitHub repository, will be extended with the following functionalities:

- generation of space-based skyplots for visualizing the relative distribution of GNSS satellites with respect to the receiver position;
- support for Receiver Independent Exchange Format (RINEX) files, including both observation data and GNSS ephemerides;
- support for Institute of Navigation (ION)-compliant metadata encoding associated with binary I/Q data batches.

Further developments are expected to arise through contributions from both individual developers and the research community.

ACKNOWLEDGEMENTS

The LuNART and LuNART-q software development was funded within the contract n. 2021-26-HH.0 ASI/Politecnico di Torino "Attivita di R&S inerente alla Navigazione GNSS nello Space volume Terra/Luna nell'ambito del Lunar GNSS Receiver Experiment". The authors would like to thank Qascom for supplying the representative datasets of LuGRE operations that supported this study.

REFERENCES

Fu, G. M., Khider, M., and Van Diggelen, F. (2020). Android raw GNSS measurement datasets for precise positioning. In *Proceedings of the 33rd international technical meeting of the satellite division of the Institute of Navigation (ION GNSS+ 2020)*, pages 1925–1937.

Hossain, E. (2022). App designer and graphical user interface in matlab. In *MATLAB and Simulink Crash Course for Engineers*, pages 299–316. Springer.

Konitzer, L., Parker, J. J., Ashman, B., Esantsi, N., Facchinetti, C., Dovis, F., Minetto, A., Nardin, A., Bauer, F., Ansalone, L., et al. (2024). Science objectives and investigations for the lunar GNSS receiver experiment (lugre). In *Proceedings of the 37th International Technical Meeting of the Satellite Division of The Institute of Navigation (ION GNSS+ 2024)*, pages 1061–1081.

Parker, J. J. K., Dovis, F., Anderson, B., Ansalone, L., Ashman, B., Bauer, F. H., D'Amore, G., Facchinetti, C., Fantinato, S., Impresario, G., McKim, S. A., Miotti, E., Miller, J. J., Musmeci, M., Pozzobon, O., Schlenker, L., Tuozzi, A., and Valencia, L. (2022). The lunar GNSS receiver experiment (LuGRE). In *Proceedings of the ION ITM 2022 Conference*, Long Beach, California. NASA and Italian Space Agency (ASI), Institute of Navigation.

Tedesco, S., Bernardi, F., Guzzi, S., Boschiero, M., Pulliero, M., Marcantonio, D., Ghedin, M., Miotti, E., Fantinato, S., Pozzobon, O., Facchinetti, C., Musmeci, M., D'Amore, G., Varacalli, G., Minetto, A., Dovis, F., Parker, J. J. K., McKim, S. A., Konitzer, L., Ashman, B., Sanathanamurthy, S., Miller, J. J., Valencia, L., and Bauer, F. (2023). Deep space GNSS in moon transfer orbit: the LuGRE receiver. In *2023 IEEE International Conference on Wireless for Space and Extreme Environments (WiSEE)*.